EFFICIENT WAVEFORM DECOMPOSITION ON AIRBORNE LASER BATHYMETRY

W. Cheng, W.-S. Lu, and A. Antoniou

Department of Electrical and Computer Engineering
University of Victoria, Victoria, B.C., V8W 3P6

ABSTRACT

A technique for the efficient processing of bathymetric data is presented. First, the characteristics of bathymetric signals are analyzed in the time domain. A bathymetric signal is characterized by three components that represent the blue-green surface reflection, volume backscatter, and bottom reflection. This characterization facilitates the decomposition of the waveform and renders the depth estimation reliable and physically meaningful. Recursive computational schemes for the evaluation of the signal model are derived. Our simulations have demonstrated that these schemes can be used in optimization-based depth estimation algorithms with reduced computation complexity.

I. Introduction

Airborne laser bathymetry is a state-of-the-art remote sensing technique utilizing laser pulses as a source for light detection and ranging (LIDAR) for depth mapping of shallow waters. For each laser sounding, a time-series waveform, representing the amount of photon energy received from the reflection of laser pulses, is collected by a laser transceiver mounted on the aircraft platform. Each of the received signals is sampled at 2-ns intervals and contains 256 consecutive samples. Depth estimation for each sounding is then carried out on the basis of the time difference between the surface and bottom reflections. Obviously, accurate identification of the reflections is of critical importance in sea depth estimation.

The work presented here is based on waveforms collected by the LARSEN 500 system, which is a Canadian airborne laser bathymeter. It transmits a series of laser pulses from an aircraft at an altitude of 500 metres into the ocean and receives the reflections from the ocean surface and floor. The system performs a circular scan across the track as it moves along the track. A typical waveform of the returning pulse energy and its four major components are illustrated in Figure 1. If the time difference between the detected surface and bottom returns, T_d, is known, the vertical water column depth can be obtained as

$$\text{depth} = \frac{T_d C}{2r} \tag{1}$$

where T_d is the time interval between the peaks of the blue-green surface and bottom reflections, as illustrated in the Figure 1, C is the speed of light in air, and r is the refractive index of sea water.

In this paper, a new parametric model which consists of three signal components representing the blue-green surface reflection, volume backscatter, and bottom reflection is proposed. This model is based on the waveform characterization and decomposition technique proposed reported in [1, 2]. The amount of computation required for the evaluation of the model functions is fairly large but through the use of a recursive algorithm, efficient evaluation of these functions can be achieved. Using this algorithm, the function value at a given sample point is obtained by multiplication of the function value at the previous sample point by a constant derived from a computation of function values at any two consecutive sample points.

II. Waveform Characterization

A. Blue-Green Surface Reflection

As we can see from Figure 1, there are two distinct surface reflections which result from the infrared and blue-green laser pulses. The appearance of the infrared surface reflection indicates a "true" surface reflection and serves as a marker between waveforms collected from two consecutive sounding positions. The infrared laser pulses of wavelength 1064 nm can only penetrate about 20 cm of the water body, while blue-green laser pulses whose wavelength is about 532 nm are much less attenuated in the water and thus can serve as an effective source for ranging and detection.

A mathematical function that can model the blue-green surface reflection is the exponentially modified Gaussian (EMG) function [1]. The function offers a variety of asymmetrical profiles that resemble the surface reflection. It is defined by the convolution of the standard Gaussian function with an exponential decay function, i.e.,

$$\begin{aligned} Y_{EMG}(t) &= h_G S_\tau e^{-T^2/2} e^{(S_\tau - T)^2/2} \int_{S_\tau - T}^{\infty} e^{-\xi^2/2}\, d\xi \\ &= h_G S_\tau e^{S_\tau^2/2 - S_\tau T} \int_{-\infty}^{T - S_\tau} e^{-\xi^2/2}\, d\xi \end{aligned} \tag{2}$$

where

$$T = \frac{(t - t_G)}{\sigma_G} \quad \text{and} \quad S_\tau = \frac{\sigma_G}{\tau}$$

0-7803-2553-2/95/$4.00

Function Y_{EMG} in (2) depends on four parameters, i.e., h_G, σ_G, τ, t_G, and the asymmetry of Y_{EMG} is determined by the peak height and peak position of Y_{EMG} which are denoted as P and t_p, respectively. From (2), the relationship between P and t_p can be expressed as

$$P = Y_{EMG}(t_p) = h_G S_\tau e^{S_\tau^2/2} e^{-S_\tau T_p} \int_{-\infty}^{T_p - S_\tau} e^{-\xi^2/2}\, d\xi$$

where t_p is the time instant when the peak of Y_{EMG} occurs and $T_p = (t_p - t_G)/\sigma_G$. Hence

$$h_G S_\tau e^{S_\tau^2/2} = P\left[\frac{e^{(t_p - t_G)/\tau}}{I_{zp}}\right] \tag{3}$$

where

$$I_{zp} = \int_{-\infty}^{z_p} e^{-\xi^2/2}\, d\xi$$

and

$$z_p = T_p - S_\tau = \frac{(t_p - t_G)}{\sigma_G} - \frac{\sigma_G}{\tau}$$

It follows that (2) can be written as

$$Y_{EMG}(t) = P\left[\frac{e^{(t_p - t)/\tau}}{I_{zp}}\right] I(z) \tag{4}$$

where

$$z = T - S_\tau = \frac{t - t_G}{\sigma_G} - \frac{\sigma_G}{\tau}$$

and

$$I(z) = \int_{-\infty}^{z} e^{-\xi^2/2}\, d\xi$$

Integral $I(z)$ in (4) can be approximated by a polynomial expression [3] as

$$I(z) = \begin{cases} A(z)\, B(q) & \text{for} \quad z \leq 0 \\ \sqrt{2\pi} - A(z)\, B(q) & \text{for} \quad z > 0 \end{cases} \tag{5}$$

where

$$A(z) = e^{-z^2/2}, \quad B(q) = \sum_{i=1}^{5} b_i q^i, \text{ and } \quad q = \frac{1}{1 + p|z|}$$

with parameters p and b_i $(i = 1, \ldots, 5)$ given by Table 1.

Table 1: Constant in polynomial approximation of (5)

Parameter	Value
p	0.231642
b1	0.319382
b2	−0.356564
b3	1.781480
b4	−1.821260
b5	1.330270

B. Bottom Reflection

The bottom reflection is affected by a number of factors such as sea turbidity, bottom reflectivity, sea state, and sea depth. For example, a sea bottom composed of rocks and sea grass can broaden the reflected pulse significantly while the dispersion effects of laser pulse in water may skew the bottom reflection. The Gaussian function is used to characterize the bottom reflection in the LARSEN waveform, i.e.,

$$Y_G(t) = A_{max} e^{-(t - t_{max})^2/2\sigma^2} \tag{6}$$

where A_{max} is the maximum amplitude of the Gaussian function, t_{max} is the instant when the maximum amplitude occurs, and σ is the standard deviation. The three parameters A_{max}, t_{max}, and σ can be adjusted to quantify amplitude, peak position, and width of the profile.

C. Volume Backscatter

In between the surface and bottom reflections, there exists a large section of the profile that represents the laser backscatter of the water column. It is usually referred as volume backscatter. It represents the interaction of laser pulses with the water body where the suspended particles and incidental materials in between the water column defract the laser light by scattering. Throughout our studies, the turbidity of the water column is assumed to be uniform. Consequently, the backscatter energy from the water column decays exponentially and causes the trailing edge of the reflection pulse to become asymmetrical. The same EMG function as in (2) can be used for the characterization of the backscatter. The significance of characterizing the volume backscatter in the course of sea depth estimation is that a large amount of backscatter from the water column sometimes shifts the peak positions of the surface and bottom reflections, which may result in unreliable depth estimates.

D. Recursive Computation of the Modeling Functions

In the process of characterization and decomposition of the waveforms into the three components, namely, surface reflection, volume backscatter, and bottom reflection, we need to find an optimal set of parameters for each characteristic function. This is done by using numerical optimization techniques to minimize the difference between sample values and the values calculated from the waveform model. In order to facilitate the efficient calculation of the values of the function at the sample points, a recursive computation scheme is developed in the next two subsections and the computation efficiency will be demonstrated thereafter.

E. Recursive Computation of the Surface Reflection

At time t_k, the EMG function can be expressed as

$$
\begin{aligned}
Y_{EMG}(t_k) &= P\left[\frac{e^{(t_p-t_k)/\tau}}{I_{zp}}\right] I(z_k) \\
&= Y_{EMG1}(t_k)\, I(z_k)
\end{aligned} \tag{7}
$$

where

$$
\begin{aligned}
z_k &= \frac{t_k - t_G}{\sigma_G} - \frac{\sigma_G}{\tau} \\
Y_{EMG1}(t_k) &= P\left[\frac{e^{(t_p-t_k)/\tau}}{I_{zp}}\right] \\
I(z_k) &= \int_{-\infty}^{z_k} e^{-\xi^2/2}\, d\xi
\end{aligned}
$$

At the next sampling instant $t_{k+1} = t_k + \Delta$, Y_{EMG} is given by

$$
\begin{aligned}
Y_{EMG}(t_{k+1}) &= P\left[\frac{e^{(t_p-t_{k+1})}}{I_{zp}}\right] I(z_{k+1}) \\
&= P\left[\frac{e^{(t_p-t_k)/\tau-\Delta/\tau}}{I_{zp}}\right] I(z_{k+1}) \\
&= Y_{EMG1}(t_k)\, e^{-\Delta/\tau} I(z_{k+1}) \\
&= Y_{EMG1}(t_k)\, C_4 I(z_{k+1})
\end{aligned} \tag{8}
$$

where

$$
C_4 = e^{-\Delta/\tau} \quad \text{and} \quad I(z_{k+1}) = \int_{-\infty}^{z_{k+1}} e^{-\xi^2/2}\, d\xi
$$

Concerning the evaluation of $I(z_k)$ and $I(z_{k+1})$, we note that using (5) one can approximate $I(z_k)$ and $I(z_{k+1})$ by polynomials of $A(z)$ and $B(q)$ at z_k and z_{k+1}, respectively. Furthermore, $A(z_{k+1})$ can be obtained recursively through the following formulas. If we let

$$
a = A(z_k) = e^{-z_k^2/2} \tag{9}
$$

then

$$
\begin{aligned}
A(z_{k+1}) &= e^{-z_{k+1}^2/2} \\
&= e^{-(z_k+\Delta/\sigma_G)^2/2} \\
&= e^{-z_k^2/2}\left(e^{-\Delta/\sigma_G}\right)^{z_k}\left(e^{-\Delta/\sigma_G}\right)^{\Delta/2\sigma_G} \\
&= a\,[C_{5,k-1}C_6]\, C_7 \\
&= a C_{5,k} C_7
\end{aligned} \tag{10}
$$

where

$$
C_{5,k} = C_{5,k-1}C_6 = \left(e^{C_8}\right)^{z_{k-1}}\left(e^{C_8}\right)^{-C_8}
$$

and

$$
\begin{aligned}
C_7 &= \left(e^{-\Delta/\sigma_G}\right)^{\Delta/2\sigma_G} \\
C_8 &= e^{-\Delta/\sigma_G}
\end{aligned}
$$

F. Recursive Computation of Bottom Reflection

The bottom return function $Y_G(t)$ can also be evaluated recursively. At time t_k, $Y_G(t_k)$ is given by

$$
Y_G(t_k) = A_{max} e^{-(t_k-t_{max})^2/2\sigma^2}
$$

If we let

$$
b = Y_G(t_k) = A_{max} e^{-(t_k-t_{max})^2/2\ sigma^2}
$$

then $Y_G(t_{k+1})$ is given by

$$
\begin{aligned}
Y_G(t_{k+1}) &= A_{max} e^{-(t_{k+1}-t_{max})^2/2\sigma^2} \\
&= A_{max} e^{-(t_k+\Delta-t_{max})^2/2\sigma^2} \\
&= b C_1 C_{2,k}
\end{aligned} \tag{11}
$$

where

$$
\begin{aligned}
C_1 &= e^{-\Delta^2/2\sigma^2} \\
C_{2,k} &= e^{-(t_k-t_{max})/\sigma^2} \\
&= C_{2,k-1}C_3 \\
C_3 &= e^{-\Delta/\sigma^2}
\end{aligned}
$$

G. Simulation Results

In terms of the number of floating-point operations used, the evaluation results obtained by implementing the recursive as well as direct computation schemes are given in Table 2. It is noted that the computational complexity is reduced by 32.97% and 19.33% for the evaluation of functions Y_{EMG} and Y_G, respectively.

Table 2: Computation complexity: recursive v.s. direct

Function	Direct	Recursive	Reduction Percentage
Y_{EMG}	10220	6850	32.97 %
Y_G	1283	1035	19.33 %

III. Waveform Decomposition

As was mentioned earlier, the waveform can be modeled mathematically as

$$
Y_T(t) = Y_{EMG}(t) + Y_G(t) + Y_{BS}(t) \tag{12}
$$

where Y_T is the lowpass-filtered waveform, Y_{EMG} is the surface reflection function, Y_G is the bottom return function, and Y_{BS} is the backscatter from the water column. In order to determine the parameters of Y_{EMG}, Y_{BS}, and Y_G, we define the objective function

$$
E(\boldsymbol{x}) = \sum_{k=1}^{m} e_k^2(\boldsymbol{x}) = e(\boldsymbol{x})^T e(\boldsymbol{x}) \tag{13}
$$

where

$$
\begin{aligned}
e_k(\boldsymbol{x}) &= e(\boldsymbol{x}, t_k) = Y_T(t) - y(t_k) \\
e(\boldsymbol{x}) &= [e_1(\boldsymbol{x}) \cdots e_k(\boldsymbol{x}) \cdots e_m(\boldsymbol{x})]^T
\end{aligned}
$$

t_k is the value of t at the kth sampling point, $y(t_k)$ represents the value of the waveform at t_k, and $Y_T(t_k)$ is defined by (12). Using optimization, $E(\boldsymbol{x})$ can be minimized with respect to parameters $\boldsymbol{x}$ [1, 2].

Several quasi-Newton optimization methods are available in the literatures [4, 5]. The Broyden-Fletcher-Goldfarb-Shanno (BFGS) method is one of the robust and efficient quasi-Newton methods, and it was found to give good results in the above minimization.

The first block of 35 samples is largely contributed by the surface reflection, since the backscatter envelop and bottom return are negligible in this range. Thus $Y_T(t)$ in (12) can be simplified as

$$Y_T(t) = Y_{EMG}(t) \tag{14}$$

By applying the BFGS optimization to the objective function defined by (13) with $Y_T(t)$ given by (14), we can determine the values of the parameters of Y_{EMG}. Having done this, we subtract the modeled surface return signal, i.e., Y_{EMG} from the smooth waveform data, which is obtained by applying a 12th-order lowpass filter [6] to the original waveform. Finally, we proceed to identify the bottom reflection by applying the BFGS method to the objective function in (13) with

$$Y_T(t) = Y_G(t) \tag{15}$$

to determine the values of the parameters for $Y_G(t)$. Figure 2 shows the plot of the three-function modeling and decomposition of the waveform in Figure 1.

IV. Conclusion

A new parametric model which consists of three signal components representing the surface reflection, volume backscatter, and bottom reflection has been proposed. It has been shown that the functions involved in the model can be efficiently evaluated by using recursive formulas.

On comparing the proposed algorithm with the existing evaluation method which computes the function values directly [1, 2], our algorithm yields a 30 percent reduction in the number of floating-point operations. Simulations have been included to illustrate the method proposed.

The information provided by the method presented may be found useful in marine engineering research in addition to sea depth estimation, for example, for the measurement of turbidity.

Acknowledgement

The authors are grateful to the Natural Sciences and Engineering Research Council of Canada and Micronet, NCE Program, for supporting this research.

References

[1] H. Wong, "Signal processing techniques for airborne laser bathymetry," Ph.D. dissertation, University of Victoria, Dec. 1993.

[2] H. Wong and A. Antoniou, "One-dimensional signal processing techniques for airborne laser bathymetry," *IEEE Trans. Geoscience and Remote Sensing,* Jan. 1994.

[3] M. Abramowitz and I. A. Stegun, eds., *Handbook of Mathematical Functions.* Applied Mathematics Series, No. 55, National Bureau of Standards, Washington, D.C., pp. 1779-1784, 1989.

[4] R. Fletcher, *Practical Methods of Optimization.* vol. 1, John Wiley, New York, 1980.

[5] A. Antoniou, *Introduction to Optimization Theory and Practice.* University of Victoria, Dept. of Elec. and Comp. Engr., Apr. 1992.

[6] A. Antoniou, *Digital Filters: Analysis, Design, and Applications.* Second Edition, McGraw-Hill, 1993.

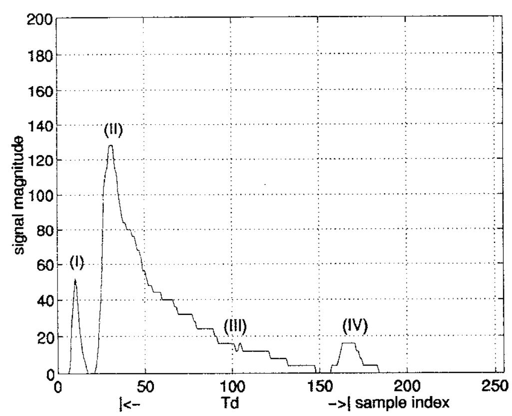

Figure 1: A typical bathymetric waveform. I: infrared surface reflection; II: blue-green surface reflection; III: volume backscatter, IV: bottom reflection.

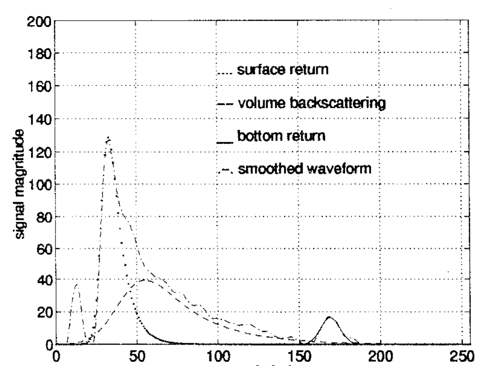

Figure 2: Decomposition of the waveform in Figure 1. The dotted line is the blue-green surface reflection, the dashed line is the volume backscatter, the solid line is the bottom reflection, and the dashdot line is the smoothed waveform.